Available online at www.sciencedirect.com
ScienceDirect
Journal of the European Ceramic Society 27 (2007) 165–171
www.elsevier.com/locate/jeurceramsoc

Raman study of yttria-stabilized zirconia interfacial coatings on Nicalon™ fiber

N.I. Baklanova [a,*], B.A. Kolesov [b], T.M. Zima [a]

[a] *Institute of Solid State Chemistry and Mechanochemistry SB RAS, Kutateladze st. 18, Novosibirsk 630128, Russian Federation*
[b] *Institute of Inorganic Chemistry SB RAS, Novosibirsk 630090, Russian Federation*

Received 23 November 2005; received in revised form 10 April 2006; accepted 21 April 2006
Available online 6 June 2006

Abstract

The undoped, 3Y- and 9Y-stabilized ZrO_2 interfacial coatings on SiC-based fiber type Nicalon™ were fabricated by sol–gel approach and studied using Raman spectroscopy. Raman spectroscopy proved to be a very successful method for revealing beyond question the monoclinic, tetragonal and cubic modification in the as-prepared and exposed to air ZrO_2-coated Nicalon™ fibers. The quantitative phase analysis in the tetragonal or tetragonal/monoclinic two-phase interfacial zirconia coatings was done using an accurate calibration curve directly determined from the Raman spectra of standard mixtures with known monoclinic and tetragonal phase ratios. It was found that the undoped ZrO_2 coating on Nicalon™ fiber was composed of monoclinic together with tetragonal modification in approximately equal fractions whereas after exposition to air the t → m phase transformation occurred in full extent. The 3YSZ coating also underwent the t → m transformation, with the extent of this transformation being different for various areas of the same filament and for various filaments.

A monitoring of the t → m phase transformation within ZrO_2 coating on Nicalon™ fiber using micro-Raman spectroscopy makes it possible quantitatively to evaluate an ability of ZrO_2 as oxidation resistance and readily deformable weak interfacial coating for CMC's.

Keywords: Interfaces; Spectroscopy; Structural applications; YSZ; ZrO_2; Coating; SiC

1. Introduction

Zirconia especially in tetragonal or cubic phase is technologically important in the engineering of advanced materials for different applications, including structural ceramics, gas sensors, fuel cells, catalysis. Zirconia is widely used as structural ceramic material for its high strength and fracture toughness originating from martensitic transformation from tetragonal to monoclinic (t → m) modification.

Recently the feasibility of using a CVD ZrO_2 fiber coating as an oxidation-resistant and weak interphase for structural composite materials such as SiC/SiC (CMC's) was proposed and thoroughly studied by Lee et al.[1–4] They found that the CVD ZrO_2 interfacial coating on Nicalon type fiber exhibited desired tensile failure behavior, extensive crack deflection within the interface region and fiber debonding (i.e. weak interface behavior). On the basis of SEM and TEM observations they proposed that the key mechanism of the delamination within ZrO_2 layer is the martensitic transformation of t-ZrO_2 nuclei to m-ZrO_2 on reaching a critical grain size and the development of significant compressive stresses due to the expansion of the cell volume and shear associated with the martensitic transformation. However, an uncertainty still exists in the explanation of reasons for delamination observed within ZrO_2 interfacial layer. Because the delamination can originate from the ZrO_2 phase transformation it would be desirable to monitor this transformation in the interfacial coating. Raman spectroscopy is very convenient technique for these purposes due to the fact that the Raman spectra of the cubic, tetragonal and monoclinic ZrO_2 modifications are strongly distinct from each other.[5]

It is well known that an addition of Y_2O_3 or other rare earth oxides results in the appearance of oxygen vacancies and the formation of the stabilized tetragonal or cubic ZrO_2 phases in dependence of dopant level.[6] Earlier it was reported the fabrication of the Y-PSZ interfacial coating on Nicalon™ fiber by sol–gel approach.[7,8] It was demonstrated that sol–gel approach

* Corresponding author. Tel.: +7 3832 363839; fax: +7 3832 322847.
E-mail address: baklanova@solid.nsc.ru (N.I. Baklanova).

0955-2219/$ – see front matter © 2006 Elsevier Ltd. All rights reserved.
doi:10.1016/j.jeurceramsoc.2006.04.151

enables accurately to control of the phase composition of an interphase zone and to fabricate the cubic, tetragonal and monoclinic ZrO_2 modifications in coating layer. The aim of this work is to study of the peculiarities of the yttria-stabilized ZrO_2 interfacial coatings on Nicalon™ fiber and phase transformations within coating layer by Raman spectroscopy.

2. Experimental procedure

2.1. Substrate and coating preparation

Woven Nicalon™ NLM202 fiber cloths (Nippon Carbon Co., Japan) were used as substrate materials. Diameter monofilament is about 15 μm. Prior to coating, Nicalon™ fiber cloths were immersed for 24 h in the 50:50 acetone/ethanol mixture for removing a sizing agent, dried at ambient temperature and thermally treated in air at 450 °C.

The coating process was based on the dipping of Nicalon™ fabrics into sols of oxide metals. The preparation of initial sols was similar to that described by Yan and coworkers.[9,10] The coating solution was prepared by dissolving yttrium nitrate hexahydrate $Y(NO_3)_3{\cdot}6H_2O$ and zirconyl chloride octahydrate $ZrOCl_2{\cdot}8H_2O$ (CG, the Hf content not more than 1%) at given molar ratio in appropriate amount of ethanol–water solution. Sols with different Y_2O_3 content were prepared. Samples derived from these sols were named after the yttria content, i.e. 3Y-ZrO_2 means 3 mol.% Y_2O_3 and 97 mol.% ZrO_2. The coating stage involved firstly the immersion of the Nicalon™ fabrics into sols, whereat the specimens were dried on air at ambient temperature and slowly heated till 960 °C in argon flow at atmospheric pressure. To increase of thickness of interfacial coating the dipping–annealing procedure was repeated several times.

Also air-dried YPS powders with 0.5, 3 and 9 mol.% Y_2O_3 content were obtained using aqueous sol–gel approach[7] to prepare of standard mixtures (i.e. mixtures with known phase ratio) for Raman measurements and to compare the Raman spectra of coatings and powders of the same composition.

2.2. Specimen characterization

The FT-Raman spectra of sol–gel derived ZrO_2 and Y-PSZ powders were recorded using a Bruker RFS 100/S spectrometer equipped with a Nd-YAG laser operating at an exciting wavelength of 1064 nm. The laser output was 100 mV. For each spectrum 100 scans were accumulated. This was sufficient to obtain spectra with low noise required for fitting procedure. Raman spectra have been normalized per gram. The 3.0 version of the Opus peak-fitting software was used for peak position and integral intensity determinations. Due to the fact that the Raman spectrum of monoclinic ZrO_2 is sharply distinguished from that of tetragonal ZrO_2 it is a possible to make the quantitative phase analysis in two-phase zirconia.

Micro-Raman spectra of the Y-PSZ coated Nicalon™ fibers were recorded using a Triplemate, SPEX spectrometer equipped with CCD spectrometric detector cooled by liquid nitrogen and microscope attachment for back scattering geometry in the 40–1700 cm^{-1} region. The 488 nm radiation from an argon laser was used for spectral excitation. All measurements were carried out using a laser power of 5 mW on sample surface. The laser beam was focused with an optical objective on spot with 2 μm diameter.

The infra red (FT-IR) spectra of sol–gel derived ZrO_2 and Y-PSZ powders were recorded as CsI pressed pellets using a Fourier IR spectrometer BOMEM MB-102 in the 200–4000 cm^{-1} range.

Morphology and elemental composition of the Y-PSZ coatings on Nicalon™ fibers were examined by scanning electron microscope (SEM LEO 1430VP), supplied by energy dispersive X-ray spectrometer (EDX, Oxford).

Thermal oxidation resistance of coated Nicalon™ fabrics was examined in air under static conditions at 1000 °C. The samples of the ZrO_2 coated Nicalon™ fabrics (100–200 mg) were placed in the preliminary heated furnace (KO-14, German) and kept during definite time intervals. Then the samples were taken out, cooled in dessicator and weighted with accuracy ±0.1 mg. A total time of testing was about 30 h.

2.3. Quantitative analysis of Raman spectra

A construction of calibration curve for the quantitative phase analysis was similar to that described by Kim et al.[11] A calibration curve was directly determined from Raman spectra of standard mixtures. Standard mixtures of 13 compositions were prepared from sol–gel derived monoclinic 0.5Y-ZrO_2 and tetragonal 3Y-ZrO_2 powders, with the range of fraction of monoclinic phase, f_m, being from 0 to 1. For each of the compositions Raman spectra were measured and the deconvolution procedure was applied to the 125–205 cm^{-1} region of spectra using OPUS3.0 software which enables to simulate a position, width and intensity of peak and to estimate the integral intensities. The integral intensity ratio, $X_m = (I_{180} + I_{190})/(I_{180} + I_{190} + I_{148})$, was calculated assuming a sloped linear baseline crossing the background level at ~125 and 205 cm^{-1}.

Hardly noticeable features at the noise level at about 180 and 190 cm^{-1} were detected in Raman spectrum of 3Y-ZrO_2 powder. The content of monoclinic phase, f_m, in the 3Y-ZrO_2 powder received by us was calculated according to equation by Kim et al.[11] and it was about 1.0%. The f_m of standard mixtures were corrected in accordance with this value. Fig. 1 shows the variation of X_m with f_m. Data points were best fitted by function:

$$\log X_m = 1.15 + \left(\frac{1}{1 + 13.15 f_m^{1.35}}\right) \log f_m.$$

3. Results and discussion

3.1. Raman spectra of powders

Raman spectra of sol–gel derived 0.5Y-ZrO_2, 3Y-ZrO_2 and 9Y-ZrO_2 powders in the 100–1000 cm^{-1} region are represented in Fig. 2a–c. As one can see, in spectrum of 0.5Y-ZrO_2 at least 13 well-defined narrow bands are detected in the 100–1000 cm^{-1} region (Fig. 2a). In accordance with data reported by Lopez et

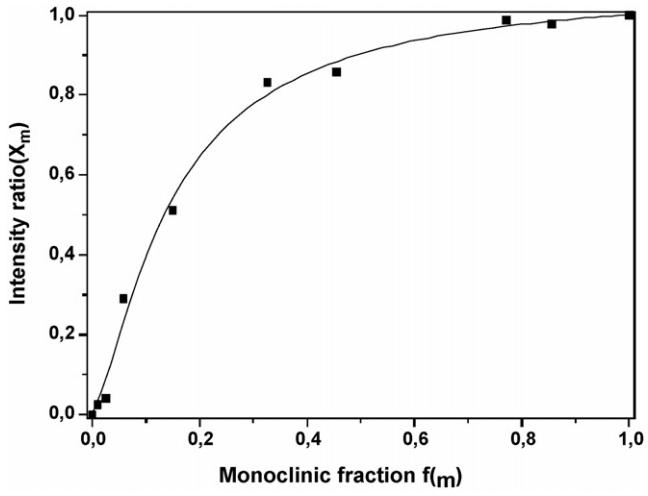

Fig. 1. Variation of the intensity ratios (X_m) with the monoclinic fraction (f_m).

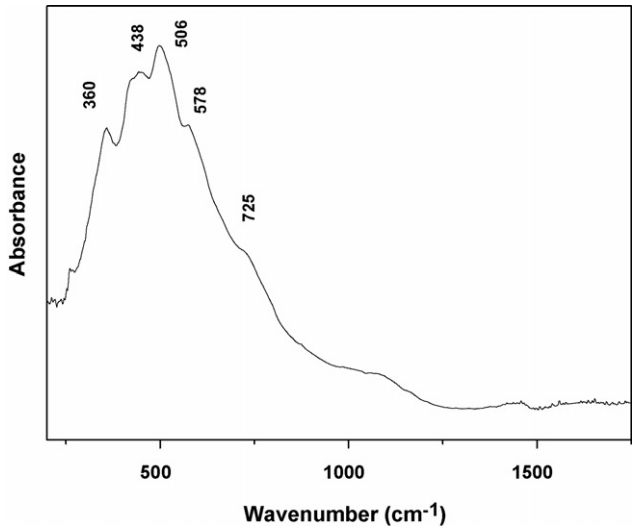

Fig. 3. IR spectrum of the 3Y-ZrO_2 powder.

al.[5], all of these bands can be assigned to monoclinic modification.

Raman spectrum of the 3Y-ZrO_2 is sharply distinct from that of 0.5Y-ZrO_2 (Fig. 2b). It clearly shows six peaks at 148 cm^{-1}, 261 cm^{-1}, 320 cm^{-1}, 466 cm^{-1}, 609 cm^{-1} (shoulder) and 641 cm^{-1}. The number and positions are in a good agreement with literature data for tetragonal modification.[5] Thus, the 3Y-ZrO_2 powder specimen is composed of tetragonal modification only. Features at the noise level were detected at about 180 and 190 cm^{-1}. They could be attributed to the strongest bands of the monoclinic zirconia impurity. The X_m calculated from Raman spectrum is about 0.044–0.054 and the corresponding f_m value is about 0.010. Thus, the m-ZrO_2 content in the as-prepared powder is not more than 1.0 wt.%. The spectra taken from the same specimens several weeks after demonstrated the stability of phase composition. The other important peculiarity of the 3Y-ZrO_2 Raman spectrum is in the fact that all of fundamentals are broadening. It can be assigned to structural disordering associated with oxygen vacancies in Y-doped samples. Additional features can be detected in the 1000–3500 cm^{-1} region, namely, small intensity bands at about 1000–1300 and 1600 cm^{-1} and very intensive and narrow band at 2860 cm^{-1} together with new features at about 2770, 3058 and 3400 cm^{-1}.

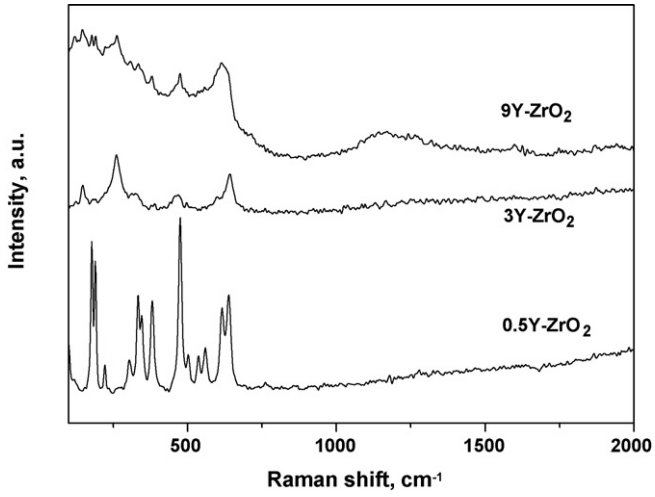

Fig. 2. Raman spectra of sol–gel derived powders.

IR spectrum of 3Y-ZrO_2 is represented in Fig. 3. Group of bands in the 300–800 cm^{-1} region is associated with IR active components of tetragonal zirconia and in good accordance with those reported for 3 mol.% Y_2O_3-stabilized ZrO_2 by Phillippi and Mazdiyasni.[12] Shoulder centered at about 725 cm^{-1} can be ascribed to the presence of m-ZrO_2.[12,13] The bands at ~1600 and 3400 cm^{-1} can be assigned to bending and stretching vibrations of H_2O molecules, respectively, which can be originated from atmospheric moisture and/or from sol–gel preparation.[12,14]

The increase of yttria content in precursor up to 9 mol.% results in the appearance of two groups of very broad peaks in Raman spectrum of powder, namely, in the 550–700 and 200–400 cm^{-1} regions (Fig. 2c). The first group is centered at about 613 cm^{-1}. This band should be assigned to the triply degenerate F_{2g} fundamental of cubic (fluorite) ZrO_2 modification. The width of this band is anomalous owing to structural disordering in the oxygen sublattice. The second very broad peak centered at about 240 cm^{-1} arises from strongly disordered structure and lowering symmetry arising from the partial substitution of Zr with Y.

Thus, Raman spectra of ZrO_2 powders with different dopant level obtained in this study demonstrate a good agreement with those reported in literature for m-, t- and c-ZrO_2.

3.2. *Micro-Raman spectra of the Y-PSZ coated Nicalon™ fibers*

Micro-Raman spectra of undoped, 3Y- and 9Y-ZrO_2 coated Nicalon™ fibers are represented in Fig. 4a–c, respectively. It should be noted that the coatings obtained for one dipping–annealing cycle were too thin for Raman spectra measurements, therefore the coatings for three dipping–annealing cycles and more were studied. One can see from Fig. 4a that the number and peak positions of the bands observed in Raman spectrum of undoped ZrO_2 are in a good agreement with data

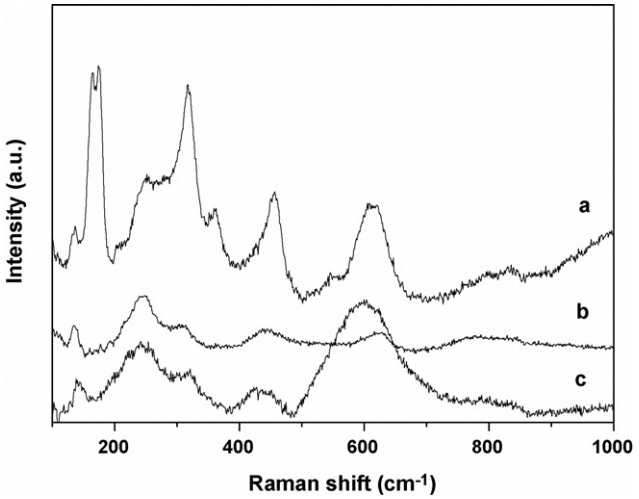

Fig. 4. Micro-Raman spectra of the ZrO_2-coated Nicalon^{TM} fibers: (a) undoped ZrO_2; (b) 3YSZ; (c) 9YSZ.

reported elsewhere for monoclinic modification. Besides, the low intensity bands at about 148 and 260 cm^{-1} which can be assigned to the strongest peaks of tetragonal modification are also present. Raman spectrum was deconvoluted into Lorentzian components in the 125–205 cm^{-1} region and integral intensity of the Raman bands were calculated. The integral intensity ratio X_m was 0.93. According to calibration curve the monoclinic fraction f_m is equal to about 0.57. So we can propose that the undoped ZrO_2 coating on Nicalon^{TM} fiber is composed of monoclinic together with tetragonal modification in approximately equal fractions. It should be noted that for $X_m = 0.8$ or more the accuracy in determining of the monoclinic fraction is poor.

The observation of metastable tetragonal ZrO_2 phase below the m–t transition temperature was reported in many works.[15–17] It was shown that the stabilization of t-ZrO_2 at low temperatures can be governed by several factors such as the crystallite size effect, the presence of stabilizers, the presence of impurities, the structural similarities between the tetragonal phase and the amorphous phase of precursor.[18(and refs therein)] Besides named factors, the influence of supports on the mechanism of tetragonal ZrO_2 phase nucleation (for coatings and films) must be taken into consideration too[19]. For example, the stabilization of t-ZrO_2 phase was observed not only for monolithic ceramic specimens but also within the CVD ZrO_2 coating on SiC fiber by Li et al.[2,3] The authors noted also that a free carbon presenting as an impurity in coating can also influence on the stabilization of the tetragonal modification. It could be proposed with discretion that the Zr–O–Si bonds the formation of which at the Nicalon^{TM} fiber/ZrO_2 coating interface was confirmed using X-ray photoelectron spectroscopy by Baklanova et al.[8] appear to be considered as stabilizing factor.

As one can see from the SEM analysis data, the 3Y-ZrO_2 coating on Nicalon^{TM} fiber (three cycles) is nonuniform one (Fig. 5a). Separate well-developed crystals and aggregates of crystals can be observed on the surface of filaments. The presence of Si, Zr, Y, O was detected by EDS micro-analysis. Micro-Raman spectra were taken from different areas of filaments including nonuniformaties (Fig. 4b). One can see that in

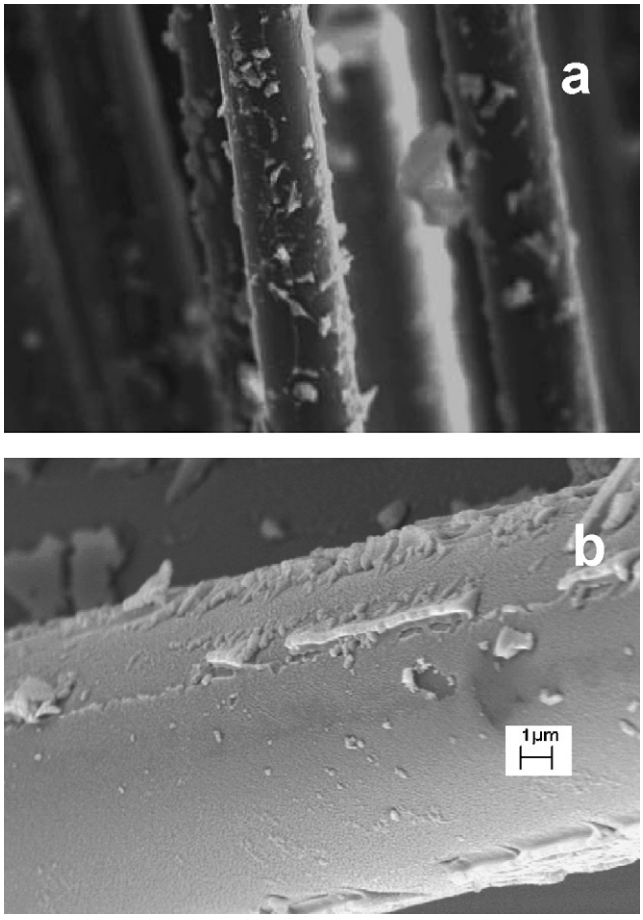

Fig. 5. SEM images of the ZrO_2-coated Nicalon^{TM} fibers: (a) 3YSZ; (b) 9YSZ.

Raman spectrum of the 3Y-ZrO_2 coating on Nicalon^{TM} fiber no any peaks other than belonging to tetragonal modification are present. As was mentioned before, monoclinic phase related bands at 178 and 190 cm^{-1} were observed in Raman spectrum of sol–gel derived 3Y-ZrO_2 powder and the content of m-ZrO_2 does not exceed 1.0 wt.%. Thus, one can note a little difference in Raman spectra of sol–gel derived 3Y-ZrO_2 powders and coatings, namely, the presence of peaks belonging to t- and m-ZrO_2 (as contamination) modifications in Raman spectrum of powders versus the tetragonal ZrO_2 peaks only in micro-Raman spectrum of coating (Figs. 2a and 4a). One could propose that the difference appears to be due to the effect of the support, namely, SiC fiber and carbon presenting on the surface of Nicalon^{TM} fiber.

Micro-Raman study of the sol–gel derived 9Y-ZrO_2 coating (two cycles and more) on Nicalon^{TM} fiber reveals very intensive asymmetric broad band at ~600 cm^{-1} (Fig. 4c). This peak can be assigned to cubic (fluorite) ZrO_2 lattice. Besides, the observed broad bands of low intensity can result from a structural disordering arising from the oxygen vacancies. The number and position of these peaks are in good accordance with those reported for fluorite-type solid solutions for YSZ.[12,13,20] One can note that Raman spectra of sol–gel derived 9Y-ZrO_2 powders and coatings obtained from the same sols are similar to each other. No any traces of monoclinic modification are detected in micro-Raman spectrum of the 9Y-ZrO_2 coating. According to SEM

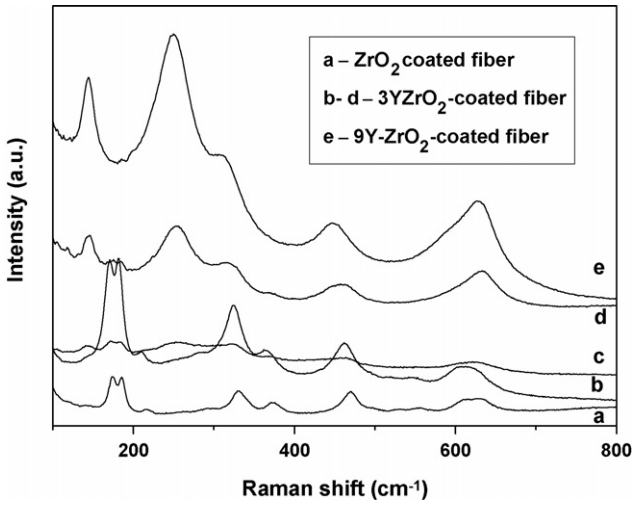

Fig. 6. Micro-Raman spectra of the ZrO_2-coated Nicalon™ fibers after the 30 h exposition to air at 1000 °C: (a) undoped ZrO_2; (b–d) 3YSZ (different areas); (e) 9YSZ.

analysis data a great number of large well-developed crystals with isometric round-shaped form and aggregates are present on the surface of filaments (Fig. 5b).

3.3. Micro-Raman spectra of the Y-PSZ coated Nicalon™ fibers after oxidation

Micro-Raman spectra of undoped ZrO_2 coating on Nicalon fiber exposed to air at 1000 °C for 30 h demonstrate only bands which can be assigned to monoclinic modification (Fig. 6a). SEM image of coating after oxidation is represented in Fig. 7. One can see that the coating is textured and built from columns which are directed normally to the surface of filament. Actually, the columnar morphology is a differential peculiarity of monoclinic modification. Thus, in despite of the fact that before oxidation the undoped ZrO_2 coating was composed of approximately half of tetragonal and monoclinic modifications, after oxidation in air for 30 h the t → m phase transformation in the coating occurred to the full extent according to micro-Raman spectra. The reason is in the fact that under heat treatment in air, the anionic vacancies in the ZrO_2 structure fill. A sufficient decrease in the number of these vacancies should facilitate instability in the metastable tetragonal phase. As a consequence, the t → m transformation is observed.[15,16] Earlier it was proposed,[2–4] that carbon particles might be a factor that can cause t-ZrO_2 stabilization. Consumption of carbon during the oxidation tests could be another plausible reason for the t → m phase transformation in the coating exposed to air. The observation of the t → m transformation for ZrO_2 interfacial coating has importance because of a highly anisotropic material, namely, monoclinic ZrO_2 is formed in course of this transformation.[21] Thus, the texture of the ZrO_2 layer can be very important variable affecting the stress state of the interphase region and the mechanical properties of composite as whole.

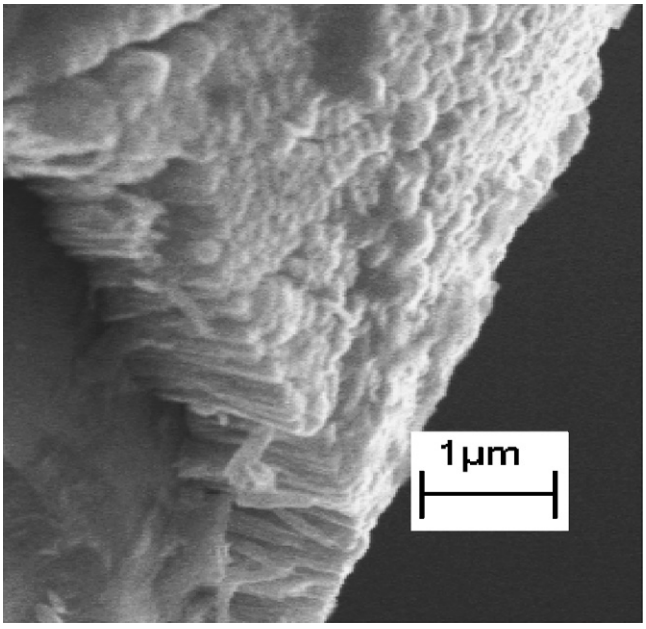

Fig. 7. SEM image of the undoped ZrO_2-coated Nicalon™ fiber after exposition to air at 1000 °C.

Under Raman microscope a clear nonuniformity of surface of the 3Y-ZrO_2 coated monofilaments can be observed. Raman spectra collected from different areas of the oxidized under the same conditions 3Y-ZrO_2 coated Nicalon™ monofilaments are shown in Fig. 6b–e. One can see that spectra are distinct from each other. The results of quantitative analysis of these spectra are listed in Table 1. One can see that there is a significant variation of monoclinic fraction (f_m) from one to another area of the surface even for the same monofilament. This can be evidence of that the different areas of coating underwent the t → m phase transformation in the different extent. One can remind that the 3Y-ZrO_2 coating contained only tetragonal modification before oxidation. One of the reasons for observable t → m transformation can be an environmental degradation of YSZ coating. Despite of rather large body literature devoted to the environmental degradation phenomenon of zirconia ceramics (see, e.g. review[22]), the nature of this process has not been yet understood. It is widely documented that zirconia ceramics stabilized with yttria, ceria, calcia or magnesia are susceptible to various environments including humid air. According to numerous studies, the mechanism of degradation is based on the formation of Zr–OH and Y–OH bonds at the surface after adsorption water; subsequently OH^- migrates into interior occupying vacancy sites, and this in turn generates a stressed region that can act as nucleating agent for the t → m transformation. Another reason for the t → m transformation within the YSZ coating on

Table 1
The X_m values determined from micro-Raman spectra of the 3Y-coated Nicalon™ fibers exposed to air at 1000 °C and corresponding monoclinic fractions

Specimen[a]	X_m	f_m
a	1	1
b	0.69	0.27
c	0.72	0.29
d	0.22	0.05

[a] Corresponds to notations in Fig. 6.

Nicalon^{TM} fiber could be the CTE fiber and coating mismatch. The repeated heating–cooling cycle during the oxidation tests results in the accumulation of stresses and as a consequence to the stress-induced the t → m phase transformation. The fact that no any transformation was detected under vacuum treatment of the YSZ coating on Nicalon^{TM} fiber during preparation is evidence in favor of an environmental degradation as dominant factor for triggering the tetragonal–monoclinic phase transformation.

As was mentioned above, there is a difference in the amount of the t → m transformation from one area to another area of the 3YSZ coating. In first turn, it can be caused by microheterogeneity of the coating, including the grains sizes, reactivity towards water vapor, a variation in composition along filament, defects, the stress level within grains. The effect of grain orientation with the respect to the laser beam polarization must be taken into account too.[23]

Micro-Raman spectrum of the 9Y-ZrO_2 coated Nicalon^{TM} fiber after oxidation demonstrates the bands which are in good agreement with those reported for 12 mol.% Y_2O_3 stabilized ZrO_2 by Feinberg and Perry.[20] The Raman band at ∼606 cm^{-1} can be assigned to a strongly disordered cubic fluorite related structure that was arose from the creation vacancies in the oxygen sublattice in the vicinity of the yttrium atoms. The rest peaks are in good agreement with those related to tetragonal distorted structure. No peaks related to m-ZrO_2 were detected in the Raman spectra of the oxidized 9Y-ZrO_2 coated Nicalon^{TM} fiber. According to Guo,[24] the cubic modification does not degrade in the environment due to its much higher oxygen-vacancy concentration on the surface. The much higher grain-boundary oxygen-vacancy concentration and the much larger grain size in the cubic ZrO_2 also ensure its stability.

4. Conclusion

It was shown in this study that sol–gel approach enables accurately to control of the phase composition of an interphase zone and to fabricate the cubic, tetragonal and monoclinic ZrO_2 modifications in coating layer on SiC-based fiber type Nicalon. To determine the phase composition of coating layer a Raman spectroscopy was used and it proved to be a very successful method for revealing beyond question the monoclinic, tetragonal and cubic ZrO_2 modifications in the as-prepared and exposed to air ZrO_2 interfacial coatings on Nicalon^{TM} fibers. The quantitative phase analysis of the tetragonal/monoclinic two-phase zirconia interfacial coatings was done using an accurate calibration curve directly determined from the Raman spectra of standard mixtures with known monoclinic and tetragonal phase ratios. On the basis of quantitative phase analysis of Raman spectra of zirconia interfacial coatings it was concluded that the as-prepared undoped ZrO_2 coating on Nicalon^{TM} fiber was composed of monoclinic together with tetragonal modification in approximately equal fractions. The exposition to air at 1000 °C of the undoped ZrO_2 coating on Nicalon^{TM} fiber led to the t → m phase transformation to the full extent. The 3YSZ coating also underwent the t → m transformation, with the extent of this transformation being different for various areas of the same filament and for various filaments. Although Nicalon type fibers with interfacial coatings are predominantly used as constituent materials for ceramic matrix composites and it is unlikely that they will be used in absence of a matrix, nevertheless the obtained results are important under the open crack conditions.

A monitoring of the t → m phase transformation within ZrO_2 interfacial coating on Nicalon^{TM} fiber using non-destructive micro-Raman technique has importance because makes it possible (i) to characterize quantitatively the behavior of the ZrO_2 interfacial coating and to evaluate its ability as an oxidation-resistant and readily deformable weak interphase for the development of non-brittle CMC's with improved strength and oxidation resistance; (ii) to establish quantitative relationships between microstructural properties of the interphase zone and mechanical properties of SiC/SiC_f composite in further studies and as consequence, to gain a better understanding of interphase role.

Acknowledgements

The authors are grateful to Dr. A.T. Titov (General Institute of Geology, Geophysics and Mineralogy SB RAS, Novosibirsk) for SEM studies and Dr. E.B. Burgina (Boreskov's Institute of Catalysis SB RAS) for IR studies and useful discussion.

References

1. Li, H., Lee, J. and Lee, W. Y., Effects of air leaks on the phase content, microstructure, and interfacial behavior of CVD zirconia on SiC fiber. *Ceram. Eng. Sci. Proc. B*, 2002, **23**(4), 261–268.
2. Li, H., Lee, J., Libera, M. R., Lee, W. Y., Kebbede, A., Lance, M. J., Wang, H. and Morsher, G. N., Morphological evolution and weak interface development within chemical-vapor-deposited zirconia coating deposited on Hi-Nicalon^{TM} fiber. *J. Am. Ceram. Soc.*, 2002, **85**(6), 1561–1568.
3. Lee, J., Li, H., Lee, W. Y. and Lance, M. J., Effects of oxygen partial pressure on the nucleation behavior and morphology of chemically-vapor-deposited zirconia on Hi-Nicalon fiber and Si. *J. Am. Ceram. Soc.*, 2003, **86**(12), 2031–2036.
4. Li, H., Morscher, G. N., Lee, J. and Lee, W. Y., Tensile and stress-rupture behavior of SiC/SiC minicomposite containing chemically vapor deposited zirconia interphase. *J. Am. Ceram. Soc.*, 2004, **87**(9), 1726–1733.
5. Lopez, E. F., Escribano, V. S., Panizza, M., Carnasciali, M. M. and Busca, G., Vibrational and electronic spectroscopic properties of zirconia powders. *J. Mater. Chem.*, 2001, **11**(7), 1891–1897.
6. Bocanegra-Bernal, M. H. and Diaz de la Torre, S., Review. Phase transformations in zirconium dioxide and related materials for high performance engineering ceramics. *J. Mater. Sci.*, 2002, **37**(23), 4947–4971.
7. Baklanova, N. I., Zima, T. M. and Titov, A. T., The oxidation resistance of the oxide-coated Nicalon^{TM} fibers. *Key Eng. Mater.*, 2005, **287**, 477–482.
8. Baklanova, N. I., Titov, A. T., Boronin, A. I. and Kosheev, S. V., The yttria-stabilized zirconia interfacial coating on Nicalon^{TM} fiber. *J. Eur. Ceram. Soc.*, 2006, **26**(5), 1725–1736.
9. Zhang, Y.-W., Yang, Y., Jin, S., Liao, C.-S. and Yan, C.-H., Long time annealing effects on the microstructures of the sol–gel-derived nanocrystalline thin films of rare earth-stabilized zirconia. *J. Mater. Chem.*, 2001, **11**(8), 2067–2071.
10. Zhang, Y.-W., Yang, Y., Tian, S., Liao, C.-S. and Yan, C.-H., Sol–gel synthesis and electrical properties of $(ZrO_2)0.85(REO_{1.5})0.15$ (RE = Sc, Y) solid solutions. *J. Mater. Chem.*, 2002, **12**(2), 219–224.

11. Kim, B.-K., Hahn, J.-W. and Han, K. R., Quantitative phase analysis in tetragonal-rich tetragonal/monoclinic two phase zirconia by Raman spectroscopy. *J. Mater. Sci. Lett.*, 1997, **16**(8), 669–671.
12. Phillippi, C. M. and Mazdiyasni, K. S., Infrared and Raman spectra of zirconia polymorphs. *J. Am. Ceram. Soc.*, 1971, **54**(5), 254–258.
13. Hirata, T., Asari, E. and Kitajima, M., Infrared and Raman spectroscopic studies of ZrO_2 polymorphs doped with Y_2O_3 or CeO_2. *J. Solid State Chem.*, 1994, **110**(2), 201–207.
14. Strekalovsky, V. N., Polezhaev, Yu. M. and Palguev, S. F., Nonstoichiometric oxides: composition, structure, phase transformation. *Science (Moscow)*, 1987, 125–126 (in Russian).
15. Collins, D. E., Rogers, K. A. and Bowman, K. J., Crystallization of metastable tetragonal zirconia from the decomposition of a zirconium alkoxide derivative. *J. Eur. Ceram. Soc.*, 1995, **15**(11), 1119–1124.
16. Tomaszewski, H. and Godwod, K., Influence of oxygen partial pressure on the metastability of undoped zirconia dispersed in alumina matrix. *J. Eur. Ceram. Soc.*, 1995, **15**(1), 17–23.
17. Stachs, O., Gerber, Th. and Petkov, V., The formation of zirconium oxide gels in alcoholic solution. *J. Sol-Gel Sci. Technol.*, 1999, **15**(1), 23–30.
18. Xu, G., Zhang, Y.-W., Han, B., Li, M.-J., Li, C. and Yan, C.-H., Unusual calcinations temperature dependent tetragonal–monoclinic transitions in rare earth-doped zirconia nanocrystals. *Phys. Chem. Chem. Phys.*, 2003, **5**, 4008–4014.
19. Baklanova, N. I., Zima, T. M., Naymushina, T. M. and Kosheev, S. V., The formation of refractory oxide coatings on Nicalon ^{TM} fiber by sol–gel process. *J. Eur. Ceram. Soc.*, 2004, **24**(10/11), 3139–3148.
20. Feinberg, A. and Perry, C. H., Structural disorder and phase transitions in ZrO_2–Y_2O_3 system. *J. Phys. Chem. Solids*, 1981, **42**(6), 513–518.
21. Touloukian, Y. S., Kirby, R. K., Taylor, R. E. and Lee, T. Y. R., *Thermal Expansion: Nonmetallic Solids*. Plenum Press, New York, 1977, p. 451.
22. Lawson, S., Environmental degradation of zirconia ceramics. *J. Eur. Ceram. Soc.*, 1995, **15**(6), 485–502.
23. Kelly, G. L. and Finlayson, T. R., Quantitative Raman spectroscopy of Mg-(PSZ) ceramics. *J. Mater. Sci.*, 1998, **33**(15), 3849–3851.
24. Guo, X., On the degradation of zirconia ceramics during low-temperature annealing in water or water vapor. *J. Phys. Chem. Solids*, 1999, **60**(4), 539–546.